Environ Monit Assess (2014) 186:8089–8107
DOI 10.1007/s10661-014-3989-x

Assessment of trace element contamination in sediment cores from the Pearl River and estuary, South China: geochemical and multivariate analysis approaches

Yongqiang Yang · Zhuli Liu · Fanrong Chen · Shijun Wu · Ling Zhang · Mingliang Kang · Jie Li

Received: 12 December 2013 / Accepted: 29 July 2014 / Published online: 28 August 2014

Abstract Twenty-four major and trace elements and the mineralogical composition of four sediment cores along the Pearl River and estuary were analyzed using ICP-AES, ICP-MS, and X-ray diffraction (XRD) to evaluate contamination levels. The dominant minerals were quartz, kaolinite, and illite, followed by montmorillonite and feldspars, while small amounts of halite and calcite were also observed in a few samples. Cluster analysis (CA) and principal component analysis (PCA) were performed to identify the element sources. The highest metal concentrations were found at Huangpu, primarily due to wastewater treatment plant discharge and/or the surreptitious dumping of sludge, and these data differed from those of other sources. Excluding the data from Huangpu, the PCA showed that most elements could be considered as lithogenic; few elements are the combination of lithogenic and anthropogenic sources. An antagonistic relationship between the anthropogenic source metals (K, Ba, Zn, Pb, Cd, Ag, Tl, and U) and marine source metals (Na, Mg, Ti, V, and Ca) was observed. The resulting normalized Al enrichment factor (*EF*) indicated very high or significant pollution of Cd, Ag, Cu, Zn, Mo, and Pb at Huangpu, which may cause serious environmental effects. Conflicting results between the PCA and *EF* can be attributed to the background values used, indicating that background values must be selected carefully.

Keywords Major and trace elements · Multivariate analysis · Enrichment factor · Core sediments · Pearl River Estuary

Introduction

Geochemical studies of sediments in rivers and estuaries have been extended in the last few decades due to the growing awareness of riverine and estuarine pollution and its effects on the ecosystem (Varol 2011; Attia and Ghrefat 2013; Ho et al. 2013). Most elements entering the aquatic environment are ultimately fixed to sediments. However, these trapped elements may be recycled back to water column where they pose a threat to aquatic ecosystems via the variation of the physicochemical characteristics of the overlying water and sediment (Kalnejais et al. 2010). Therefore, sediment cores provide an archive of historical input and output of various elements within both the river and estuary ecosystems. The collected geochemical information of various elements not only provides an insight into the past

Y. Yang · Z. Liu · F. Chen (✉) · S. Wu · M. Kang · J. Li
Key laboratory of Mineralogy and Metallogeny, Guangzhou Institute of Geochemistry, Chinese Academy of Sciences,
Guangzhou 510640, China
e-mail: frchen@gig.ac.cn

Z. Liu · J. Li
University of Chinese Academy of Sciences,
Beijing 100049, China

L. Zhang
CAS Key Laboratory of Tropical Marine Bio-resources and Ecology, South China Sea Institute of Oceanology, Chinese Academy of Sciences,
Guangzhou 510301, China

and present environmental quality of the system but also serves as a baseline for future investigations (Badr et al. 2009). In recent years, many studies have achieved success in using sediment cores to establish the effects of anthropogenic and natural processes on depositional environments in different water areas (Lavilla et al. 2006; Chatterjee et al. 2007; Harikumar and Nasir 2010; Tue et al. 2012).

Being the second largest river system in southern China and a major waterway, the Pearl River Estuary (PRE) is known as one of the most industrialized and urbanized regions in China and has been, and remains, subject to significant anthropogenic influences, including vast industrial, agricultural, and municipal activities around the estuary and along the river (Pan and Wang 2012). The PRE has been a hot spot for research in recent decades (Li et al. 2000; Liu et al. 2003; Ip et al. 2007; Zhou et al. 2009; Yu et al. 2010, 2012). Because of the heavy metal toxicity to aquatic and benthonic organisms and the subsequent effects on humans, the geochemical behavior and pollution assessment of heavy metals account for a large fraction of these studies. Experiments have been demonstrated that ascending salinity promotes Cd desorption from sediments and hence increases total Cd concentrations in the water column and Cd uptake by organisms (Greger et al. 1995; Du Laing et al. 2009). However, the geochemistry of major and trace elements in sediment cores combining the upstream and downstream Pearl River and estuary with a salinity gradient is unclear. Areas around rivers and estuary environments represent zones of interaction and transition between the two systems where geochemical and sedimentological processes are highly variable both spatially and temporally. These processes determine the destination of various elements in these aquatic environments. Therefore, a comparison study of the geochemistry of various elements in sediments from the river and the adjacent estuary is important not only to understand their natural and anthropogenic origin but also to evaluate their pollution status.

The objectives of this study are the following: (1) to determine locational and vertical variations of major and trace elements along the estuary of the Pearl River, (2) to identify the source of elements based on cluster analysis and principal component analysis, and (3) to evaluate trace element contamination using enrichment factors.

Materials and methods

Study area and sampling procedures

The Pearl River is the 13th largest river in the world in terms of freshwater discharge with an annual average of 3.26×10^{11} m^3 year^{-1}. At the end of the water course, the river divides into three main tributaries, namely East River, West River, and North River (Fig. 1). The Lingdingyang estuary, also known as the PRE, receives approximately 53 % of the freshwater flow from four outlets: Humen, Jiaomen, Hongqilimen, and Hengmen (He et al. 2010). A main stream of the Pearl River, named as Major Pearl River, and its estuary were chosen for sampling (Fig. 1). The Major Pearl River has a total length of 128 km and is divided into two waterways, the Guangzhou channel (the upper reach), with a length of 78 km, an average width of 431 m, and an average water depth of 4.78 m, and the Shiziyang channel (the lower reach), which is 50 km long, about 2,200 m wide, and 6.64 m in water depth (Mai et al. 2001). The Shiziyang channel receives inflows from the Guangzhou channel and the East River and runs across an area, Panyu and Dongguan, where agriculture and industry are well developed, draining into the Lingdingyang via the Humen outlet (Fig. 1).

Site 1 is located in Huangpu District and is the locus where the Pearl River flows out to the main urban area of Guangzhou (Fig. 1). Site 2 is located adjacent to Nizhou Village and near the East River south tributary. Site 3 is located at the Humen outlet and is the locus where the Pearl River flows into the estuary. Site 4, lying in the middle shoal of the PRE and near Neilingding Island, represents a moderate pollution location influenced by the four eastern discharge outlets. Four sediment cores from sites 1, 2, 3, and 4 were collected in 2007 (Fig. 1). Sediment cores 1 (22 cm in length), 2 (48 cm in length), and 3 (39 cm in length) were sliced every 3 cm from the top to the bottom. Sediment core 4 (55 cm in length) was sliced every 2 cm from the top to 40 cm depth, and then only two 2-cm subsamples were sliced namely 46–47- and 53–54-cm subsamples. After slicing, the subsamples were stored in sealed polyethylene bags and frozen at −20 °C until analysis.

Sample preparation, analyses, and quality control

The temperature, salinity, pH, dissolved oxygen (DO), and turbidity of the overlying water were determined in

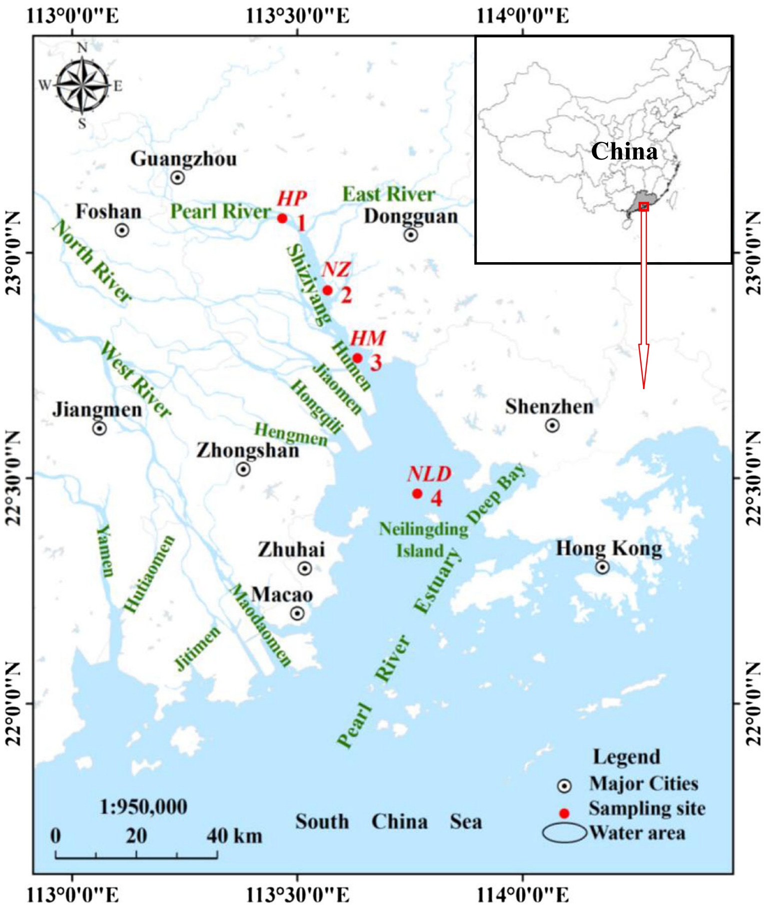

Fig. 1 Map showing the location of the study area and sediment-core collection sites on the Pearl River and estuary

situ using the YSI 6600 V2 Songde water quality monitoring system (YSI Incorporated, USA) (Table 1).

Sediment samples were freeze-dried and ground to <74 μm for the subsequent analysis. The loss on ignition (LOI) following combustion at 550 °C for 4 h was used as a proxy for organic carbon (OC) content in the sediments. Powder X-ray diffraction (XRD) was performed using an automatic Bruker D8 ADVANCE, with a Cu target tube. Diffractograms were recorded at 0.01° of the 2θ step, with an acquisition time of 3° min^{-1} at 40 kV and 40 mA.

A microwave-assisted digestion method was used to achieve total dissolution of the sediment. The following two-stage digestion procedure was employed. Approximately 150 mg of the sediment was accurately weighed in microwave vessels, and then 6 ml HNO_3 and 1.5 ml HF were sequentially added. The samples remained in contact with the acid solution for 30 min. Then, the vessels were sealed, placed in the microwave oven, and heated at rated output power (900 W) for 15 min. After cooling the vessels, 8 ml of a saturated boric acid solution was added in the second stage of the digestion. The vessels were again placed in the microwave oven and heated for 10 min at 900 W. The obtained clear solutions were poured into 120-ml HDPE bottles and diluted to 100 g. For each set of measures, digested blanks were prepared in the same manner.

A certified reference standard sediment (MESS-3) was used to test the analytical and instrument accuracy of the method. The results indicated good agreement between certified and analytical values (Table 2). Moreover, reagent blank and replicate samples were randomly inserted into the analysis procedure. The relative standard deviations of all replicate samples were less than 10 %.

Enrichment factor

Enrichment factor (*EF*) can be used to discriminate if the observed metal concentration in marine sediments is influenced by anthropogenic sources (Celis-Hernandez

Table 1 Sampling locations, water depth, and the environmental water parameters

Sites	Location (N/E)	Temperature (°C)	Salinity (‰)	pH	Dissolved O_2 (mg l^{-1})	Turbidity (N.T.U.)	Depth (m)
1	23.07667/113.46667	20.77	2.09	7.52	6.02	16.80	14.5
2	22.91667/113.56667	20.22	7.83	7.57	2.16	19.99	14.8
3	22.76667/113.63333	20.24	14.06	7.87	4.60	13.68	10.6
4	22.46667/113.76667	20.74	25.19	7.82	5.73	7.20	6.4

N.T.U. nephelometric turbidity unit

et al. 2013). The *EF* was calculated using the following equation:

$$EF = (C/B)_{sample}/(C/B)_{background}, \qquad (1)$$

where $(C/B)_{\text{sample}}$ is the ratio of the examined element concentration to the reference element concentration for the sample and $(C/B)_{\text{background}}$ is the respective baseline ratio. According to Sutherland (Sutherland 2000), $EF<2$ indicates no or minimal pollution, $2\leq EF<5$ indicates moderate pollution, $5\leq EF<20$ indicates significant pollution, $20\leq EF<40$ indicates very strong pollution, and $EF\geq 40$ indicates extreme pollution.

Table 2 Reference and determined element concentrations in the analyzed marine sediment reference materials (MESS-3)

Element		Determined values						Reference values	Recovery (%)
		1	2	3	4	5	Mean		
Al	mg g^{-1}	88.1	94.0	90.0	87.6	85.5	89.1	85.9	103.7
Fe		43.2	46.0	42.7	42.5	41.3	43.2	43.4	99.5
K		29.0	30.9	30.1	28.5	28.0	29.3	26.0[a]	112.7
Mg		18.4	19.5	18.9	18.4	17.8	18.6	16.0[a]	116.3
Na		15.9	17.2	16.4	15.9	15.4	16.2	16.0[a]	101.3
Ca		14.7	15.7	14.7	14.5	14.3	14.8	14.7	100.7
Ti		4.0	4.4	4.2	4.2	4.0	4.1	4.4	93.2
P		1.2	1.2	1.2	1.2	1.2	1.2	1.2[a]	100.0
Ba	μg g^{-1}	976	1,040	1,010	986	960	994	NA	NA
Mn		311	334	337	316	316	323	324	99.7
V		247	263	243	246	238	247	243	101.6
Sr		136	145	136	133	133	137	129	106.2
Zn		157	166	162	158	156	160	159	100.6
Cu		32.4	34.9	34.0	32.4	31.9	33.1	33.9	97.6
Cr		95.4	103	101	96.6	93.8	98.0	105	93.3
Ni		42.6	51.5	54.0	47.9	44.5	48.1	46.9	102.5
Co		15.3	14.9	16.5	15.7	15.4	15.6	14.4	108.3
Pb		19.3	20.1	20.1	19.8	19.2	19.7	21.1	93.4
Li		72.6	71.0	86.5	85.4	69.9	77.1	73.6	104.8
Mo		2.86	2.74	2.90	2.69	2.72	2.78	2.78	100.0
U		3.41	3.60	4.17	4.08	3.76	3.80	4[a]	95.0
Tl		0.84	0.81	0.97	0.94	0.86	0.88	0.90	97.8
Cd		0.25	0.26	0.25	0.24	0.24	0.25	0.24	104.2
Ag		0.20	0.21	0.20	0.20	0.18	0.20	0.18	111.1

NA not available

[a] Information value only

Statistical analysis

Multivariate statistical analysis can help simplify and organize large datasets to provide meaningful insight (Chen et al. 2007). Cluster analysis (CA), which can reveal specific linkages between sampling sites because it provides an indication of similarities or dissimilarities between their trace metal contaminations (Simeonov et al. 2000), was performed on the normalized dataset (z-scores) using Ward's method with squared Euclidean distances. Principal component analysis (PCA) is a statistical technique used to verify and quantify interrelationships among the original variables in a dataset. This procedure reduces large datasets to summary variables which account for a majority of the variability in the original dataset. All statistical data processing in this work were carried out using SPSS software (version 15.0 for Windows).

Results and discussion

Geochemistry of major elements in sediments

Major element concentrations in the investigated cores varied within the range 6.75–13.6 % for Al and 3.00–6.12, 0.35–0.76, and 0.043–0.26 % for Fe, Ti, and P, respectively (Table 3). Al and Fe had slightly elevated values compared with those of Pearl River system sediments and the average upper crust. Moreover, Al and Fe concentrations were higher at site 1 than at the other sites.

The mean values of Ca were 0.63, 0.24, 0.59, and 0.35 % at sites 1, 2, 3, and 4, respectively, far less than the average upper crust (3.00 %). This indicates that Ca is strongly depleted when compared with the average upper crust and other study areas (Table 3). Moreover, Ca was lower at site 2 than at the other sites. The Pearl River consists of three main rivers: the West River, the East River, and the North River (Fig. 1). The average concentrations of Ca were 1.12, 0.76, and 0.43 % in the West River, North River, and East River sediments, respectively (Zhang and Wang 2001). The West River basin is dominated by limestone, whereas the East River drains the South China granite area (Zhang and Wang 2001). Fe, Ca, and Mg were relatively depleted, and Al was relatively enriched in the East River sediments compared to those in the West River sediments. Site 2 is primarily controlled by the East River tributary. Moreover, site 3 is influenced by all the three River tributaries, which potentially resulted in the lowest Ca concentration at site 2. In comparison, the Ca vertical profile has large fluctuations; the highest value (1.13 %) was found at site 3 (Fig. 2), suggesting that some Ca in the core sediments was of biogenic origin, apart from the detrital contribution.

Na concentrations increased from upstream (0.31–0.47, 0.44–0.75, and 0.68–1.01 % at sites 1, 2, and 3, respectively) to the estuary (0.90–1.35 % at site 4), which were consistent with the salinity results of the overlying water (Table 1). The river discharge in the Pearl River Delta is greatly affected by the monsoonal climate and characterized by distinct changes between dry (from November to March) and wet (from May to October) seasons, with approximately 80 % water discharging in the wet season (Yin et al. 2004; Gong et al. 2013). Salt intrusion in the wet season is largely suppressed by a large amount of river inflow, while the 5 ppt isohaline can extend 80 km landward from the estuary's mouth during the dry season (Gong et al. 2013). Mg and K exhibited relatively constant values in the four cores. Na and Mg were more depleted when compared with the average upper crust. K concentrations were comparable to those in Ria de Vigo sediments (2.40–3.08 %) and the average upper crust (Table 3).

Mineralogical composition in sediments

The XRD spectra are recorded for the selected subsamples to determine the mineralogical composition. Semiquantitative calculations of the mineral percentages are made by peak surface measurements after background substraction. It should be noted that the percentages of kaolinite are actually the mixture of kaolinite and chlorite because the further methods, such as thermal and acid procedures or treatment with dimethylsulphoxide, are not conducted in this study (Gonzalez-Garcia and Sanchez-Camazano 1968). As shown in Fig. 3 and Table 4, the minerals of subsamples were dominated by quartz (25.6–50.4 %) with an average of 33.0 %, followed by kaolinite (15.2–34.3 %) and illite (11.7–25.5 %) with averages of 24.9 and 17.5 %, respectively. Montmorillonite and feldspars were observed in most subsamples with averages of 14.8 and 8.5 %, while small amounts of calcite, halite, and dolomite were only found in a few subsamples. Moreover, heavy minerals such as pyrite, goethite, and hematite cannot be identified in the four cores, which is probably

Table 3 Summary of major elements in the four sediment cores from the Pearl River and estuary

Sites		Al	Fe	K	Mg	Na	Ca	Ti	P	LOI
1	Min.	10.6	5.30	2.37	0.69	0.31	0.49	0.50	0.21	7.81
HP	Max.	12.7	6.10	2.63	0.76	0.47	0.73	0.56	0.26	9.11
	Mean	11.9	5.69	2.49	0.73	0.36	0.63	0.53	0.24	8.48
2	Min.	7.10	3.00	2.56	0.46	0.44	0.17	0.35	0.048	3.50
NZ	Max.	13.6	5.88	3.06	0.98	0.75	0.29	0.62	0.091	7.67
	Mean	10.5	4.56	2.84	0.75	0.53	0.24	0.50	0.073	6.05
3	Min.	7.56	4.27	2.19	0.68	0.68	0.32	0.50	0.054	4.24
HM	Max.	12.8	6.12	3.05	1.12	1.01	1.13	0.76	0.080	8.06
	Mean	9.96	5.15	2.52	0.94	0.79	0.59	0.65	0.069	6.16
4	Min.	6.75	3.64	2.03	0.68	0.90	0.20	0.41	0.043	5.42
NLD	Max.	11.6	5.65	2.54	1.04	1.35	0.64	0.71	0.073	8.58
	Mean	9.82	4.88	2.30	0.93	1.13	0.35	0.59	0.063	7.13
(1)	Mean	4.77	3.39	1.14	0.99	1.29	3.77	0.09	0.16	8.4
(2)	Mean	5.39	NA	0.95	5.15	1.03	6.52	NA	0.29	NA
(3)	Mean	8.24	4.96	1.84	0.83	1.02	1.12	0.68	0.081	NA
(4)	Mean	7.84	4.21	1.95	0.73	0.93	0.76	0.52	0.066	NA
(5)	Mean	9.93	3.96	2.18	0.53	1.07	0.43	0.53	0.067	NA
(6)	Mean	9.70	4.62	2.19	0.85	0.71	0.41	0.54	0.068	7.8
(7)	Range	1.21–3.84	1.16–4.29	0.71–1.73	0.03–0.26	0.21–1.08	0.22–7.78	0.17–0.75	NA	NA
(8)	Range	3.37–11.43	2.48–6.17	1.07–2.45	0.23–1.17	NA	0.21–5.31	NA	0.020–0.082	NA
(9)	Baseline	8.04	3.50	2.80	1.33	2.89	3.00	0.41	0.07	NA

All values in wt%

Medway Estuary (Reid and Spencer 2009) (*1*); Gulf of Mannar (Jonathan et al. 2004) (*2*); The West River in the Pearl River system (Zhang and Wang 2001) (*3*); The North River in the Pearl River system (Zhang and Wang 2001) (*4*); The East River in the Pearl River system (Zhang and Wang 2001) (*5*); The Pearl River Estuary (Heise et al. 2010) (*6*), (Woods et al. 2012) (*7*), and (Qi et al. 2010) (*8*); and Average upper crust (McLennan 2001) (*9*)

LOI loss on ignition, *NA* not available

due to the low level of these minerals (Seddique et al. 2011).

The estuarine subsamples contained more quartz and less illite compared with the subsamples from the Pearl River. Meanwhile, the subsamples at site 1 and subsamples 2–39 possessed high contents of clay minerals (illite, montmorillonite, and kaolinite) but low contents of quartz. It might be the reason that the concentrations of Al, Fe, Ti, Cr, Ni, and V were higher than other elements in these subsamples. Previous study has clearly indicated that the sediment-associated clay minerals do play a significant role in the adsorption of heavy metals, although this role was less significant than Fe/Mn oxides and organic materials (Wand and Li 2011). Feldspars appeared in varying percentages in all studied subsamples, and the maximum was found at site 2. As discussed above, the East River drains the south China granite area, and this rock consists mainly of feldspar and quartz, which may contribute to the high feldspars in sediments from site 2. Halite was identified only at site 4, which was contributed to the high salinity in the estuary. The maximum Ca (1.13 %) was found in subsamples 3–9, the only subsample containing calcite. The largest sum of quartz and feldspar (65.9 %) was found in subsamples 2–15, which may act to dilute the contents of other elements (e.g., Fe, Al, Na, Cr, and Zn), leading to very low concentrations of these elements (Figs. 2 and 4). In contrast, K had a higher concentration in this subsample, which was much different from other elements primarily because it is the main constituent of K-feldspar.

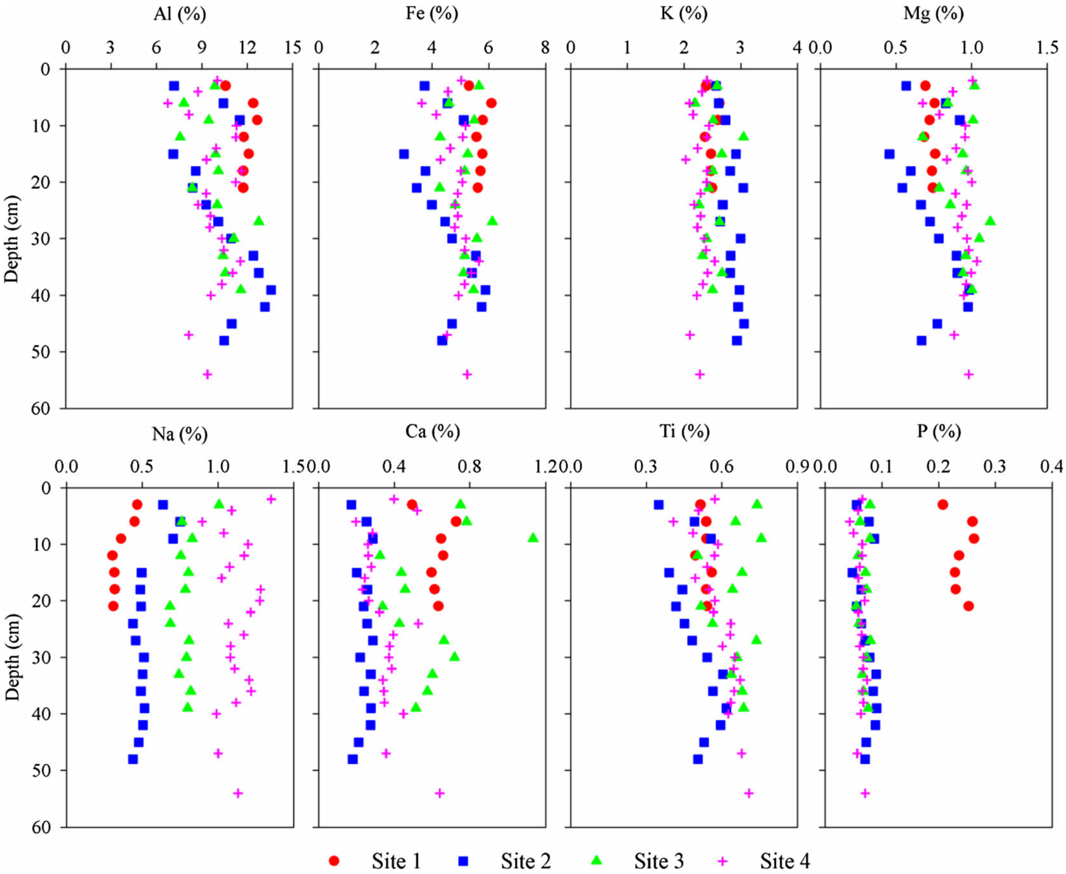

Fig. 2 Vertical profiles of major elements in the sediments from the Pearl River and estuary

Geochemistry of trace elements and Mn in sediments

Mn was the most abundant metal at sites 2, 3, and 4, while Zn had the highest concentration at site 1 (Table 5). Similar to Ca, Mn showed minimum content in the surface layer of core 2 and maximum concentration in core 3, which could be due to the distribution of Mn in the East River and West River, respectively. Other research also has shown that Mn concentrations are highest in the area between Zhuhai and the Hongqimen Gate, which is mainly controlled by the West River tributary (Woods et al. 2012). The average trace element concentrations were in the following sequential order at site 1: Zn>Mn>Ba>Cu>Cr>Pb>V>Ni>Sr>Li>Co>Mo>U>Cd>Ag>Tl, which was much different than the other cores.

The average concentrations of Ba, Ni, Cr, Mo, Pb, Cu, Zn, U, Cd, Ag, and Tl were much higher at site 1; the mean concentrations of Mn, V, Sr, Co, and Li were comparable to those at other sites (Fig. 4). Moreover, nine of the trace elements (Ba, Ni, Cu, Pb, Zn, U, Cd, Ag, and Tl) clearly decreased from upstream to the estuary, which was contrary to the Na distribution. The elevated concentrations of Zn, Cu, Pb, and Cd at site 1 were higher by a factor of two to three compared to adjacent sites (Wang et al. 2011), much greater than those in the Pearl River Estuary (Chen et al. 2012). However, they were comparable to those in the municipal sewage sludges (Fig. 5). Furthermore, it is noteworthy that the maximum concentrations of Zn (1,450 μg g^{-1}), Cu (758 μg g^{-1}), Pb (221 μg g^{-1}), and Cr (232 μg g^{-1}) at site 1 have never been reported in this area.

The Dashadi wastewater treatment plant is situated west of the Huangpu Wenchong Shipyard, south of Huangpu East Road, with a proposed daily treatment capacity of 0.2 million tons. Site 1 is located between Dajisha Island and the Huangpu Bridge, within approximately 2 km of the Dashadi wastewater treatment plant. Therefore, the elevated trace metals in core 1 were considered as the anthropogenic contaminations primarily related to the discharge from the Dashadi wastewater

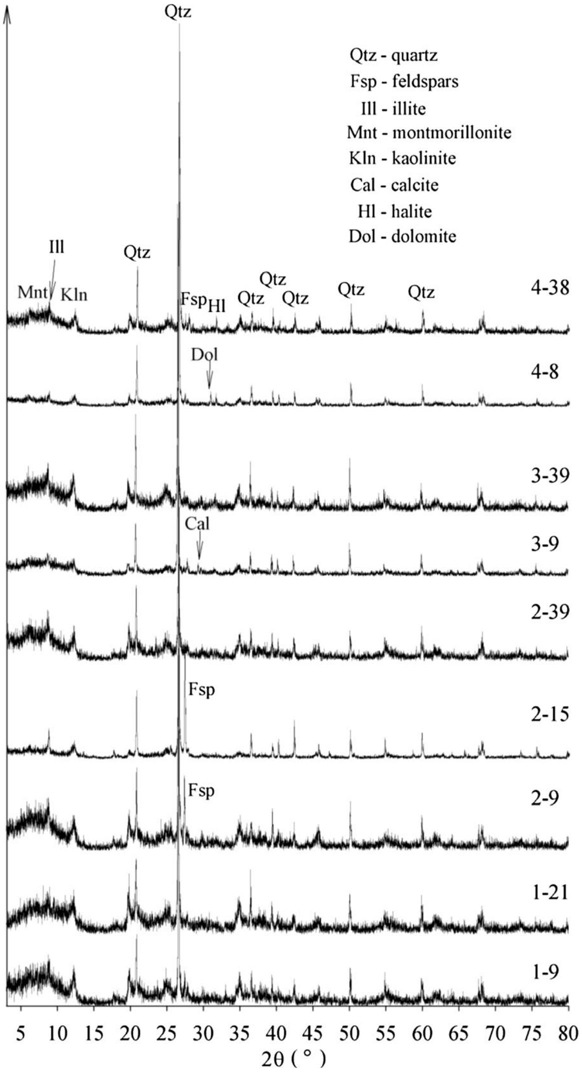

Fig. 3 X-ray diffraction patterns showing the main minerals found in selected bulk samples. Sample numbers (4–38): the 4 and 38 represent the sampling sites and the sample depth, respectively

treatment plant. For example, the median concentrations of Cd, Cu, Zn, and Pb were higher by a factor of 6–24 in sediment cores from the site nearest to the sewage treatment plant outlet than from the site located in the central part of Lake Geneva, which is as far as possible from direct human influences (Loizeau et al. 2004). A previous study confirmed that the highest Cu, Pb, and Zn concentrations (204, 332, and 2,460 μg g^{-1}, respectively) in fluvial sediment were associated with discharge from a sewage treatment plant (Birch et al. 2001). In addition, research has shown that the average trace metal contents in sewage particulate matter samples from the Malabar effluent in Sydney were 24.9, 176, 819, 97, and 1,190 μg g^{-1} for Ag, Cr, Cu, Pb, and Zn (Matthai et al. 2002). Therefore, sewage-derived heavy metals are the main contaminants in sediment from the site adjacent to the sewage treatment plant. These contaminants rapidly decrease as the distance to the outlet increases. A lot of researches have also reported high concentration of heavy metals in sewage sludge from different wastewater treatment plants (Yuan et al. 2011; Filipovic et al. 2013). Another possible reason for elevated trace metals in core 1 is the surreptitiously dumping of sludge into the Pearl River as reported by a local newspaper (NFDaily 2012), even though it is forbidden by Chinese law.

The maximum value for Li (97.4 μg g^{-1}) and the minimum values for V, Sr, and Co (64.4, 53.3, and 10.8 μg g^{-1}, respectively) were recorded in core 2, mainly attributed to the distribution of these metals in the three tributaries (the East, West, and North Rivers). Similar to Ca, the average concentrations of V (89 μg g^{-1}), Sr (51.7 μg g^{-1}), and Co (14.0 μg g^{-1}) were the lowest in the East River sediments, while the average Li content (43.1 μg g^{-1}) was the highest in the sediment of this tributary (Zhang and Wang 2001). In addition, the average values of Li were much higher in the four cores than in the three tributaries (40.1 μg g^{-1}) (Zhang and Wang 2001) and the average upper crust (20 μg g^{-1}) (McLennan 2001) but were comparable to those in the Pearl River Estuary (55.50–73.55 μg g^{-1}) (Qi et al. 2010; Woods et al. 2012). Apart from core 1, the Mo concentrations were comparable to the average upper crust values (1.5 μg g^{-1}), slightly higher than those in the Pearl River Estuary sediments (1.0 μg g^{-1}) (Woods et al. 2012) and lower than those in the Pearl River system sediments (2.47 μg g^{-1}) (Zhang and Wang 2001). The concentrations of Cu, Pb, Zn, Cd, and Ag were much higher in core 2 than in cores 3 and 4. Meanwhile, the lower value of DO and higher value of turbidity were also recorded at site 2 (Table 1), which was consistent with the previous study (Dai et al. 2006). The persistent hypoxia in upstream of the channel in Guangzhou caused by organic pollution and nitrification was demonstrated (Luo 2002). Therefore, the higher values of trace metal in core 2 might be attributed to the water pollution.

The vertical distribution of trace metals in the four cores showed distinct differences. In core 1, most trace metal concentrations increased toward the surface with a peak at 6 cm and then decreased low contents at 3 cm,

Table 4 Semiquantitative XRD mineralogy of selected bulk samples in four cores from the Pearl River and estuary

Sample name	Quartz	Feldspars	Illite	Montmorillonite	Kaolinite	Calcite	Halite	Dolomite
1–9	25.6 %	10.3 %	13.4 %	21.5 %	29.2 %	–	–	–
1–21	29.4 %	–	20.7 %	20.5 %	29.4 %	–	–	–
2–9	25.7 %	17.2 %	18.8 %	11.6 %	26.8 %	–	–	–
2–15	34.2 %	31.7 %	18.9 %	–	15.2 %	–	–	–
2–39	26 %	–	25.5 %	29.8 %	18.6 %	–	–	–
3–9	42 %	–	17.6 %	13.1 %	24 %	3.3 %	–	–
3–39	27.7 %	4.9 %	18.7 %	14.4 %	34.3 %	–	–	–
4–8	50.4 %	7.5 %	12.6 %	–	23.9 %	–	1.8 %	3.8 %
4–38	35.7 %	4.9 %	11.7 %	22.6 %	22.3 %	–	2.8 %	–

Sample numbers (1–9): the 1 and 9 represent the sampling sites and the sample depth, respectively

while Cd and Ag concentrations increased in the top 15 cm, followed by a period of lower levels (Fig. 4). Uranium exhibited a slight decreasing trend with depth and had the highest concentrations at 3 cm (10.7 μg g^{-1}). In core 2, most metals generally increased downward from 0 to 9 cm, dropped significantly at depth of 15 cm, and then increased again to ~40 cm, where the highest contents of metals were recorded. Mn, V, Sr, Ni, Cr, Co, and Li in cores 3 and 4 showed relatively large fluctuations, while other trace metals, especially Cu, Zn, Cd, and Ag, exhibited almost constant trend.

Multivariate statistical analysis

Cluster analysis

In the current study, CA was applied for the bulk sediments to look for groups of subsamples in the four cores according to their similarities. The examined data matrix included the concentrations of major and trace elements in the bulk sediments. The result obtained is presented in a dendrogram (Fig. 6), where all 57 subsamples were classified into three statistically significant clusters. The subsamples in these clusters had similar pollution level and/or sources.

The character of sediment samples in cluster 1 (all belonging to core 1) was quite different from the other two clusters, because of their very high trace metal concentrations (Fig. 4). This cluster was obviously categorized as highly contaminated sediments. As illustrated above, core 1 was characterized as a wastewater- or sludge-contributed site. The second cluster might be regarded as less contamination level due to these subsamples that had a slightly lower level for major elements and significantly lower contents for trace elements. The other subsamples, which all belonged to the cluster 3, might be explained as the moderate pollution level.

Principal component analysis

Core 1 was characterized as a wastewater- or sludge-contributed site, which is very different than the other cores. Therefore, the data at sites 2, 3, and 4 were analyzed using PCA. Major and trace elements and LOI in cores 2, 3, and 4 were further investigated by applying PCA to obtain an overview of their behaviors and possible metal sources. Two factors of the principal components were extracted that described 77.3 % of the cumulative variance (Fig. 7). Factor 1 accounted for 48.0 % of the total variance and had strong positive loadings (>0.70) of Al, Fe, P, Mn, Sr, Li, Cr, Co, Ni, Cu, Zn, and U and moderate positive loadings of Mg, Ti, Ba, V, Pb, Tl, and Mo. Usually, Al, Fe, and Mg are the major constituents of common silicate minerals. Moreover, Al held in the lattice of aluminosilicate minerals is extremely immobile in the marine environment (Qi et al. 2010). Therefore, this factor represents the lithogenic origin from weathering and erosion of rocks and soil materials in the Pearl River catchment.

Factor 2, which accounted for 29.3 % of the total variance, was distinguished by highly positive loadings of Na (0.845), Mg (0.763), Ti (0.686), V (0.682), Ca (0.542), and LOI (0.531). In contrast, K (−0.809), Cd (−0.774), Ag (−0.731), Ba (−0.687), Tl (−0.668), Zn (−0.618), U (−0.599), and Pb (−0.506) showed highly negative loadings for factor 2. The main source of Na to

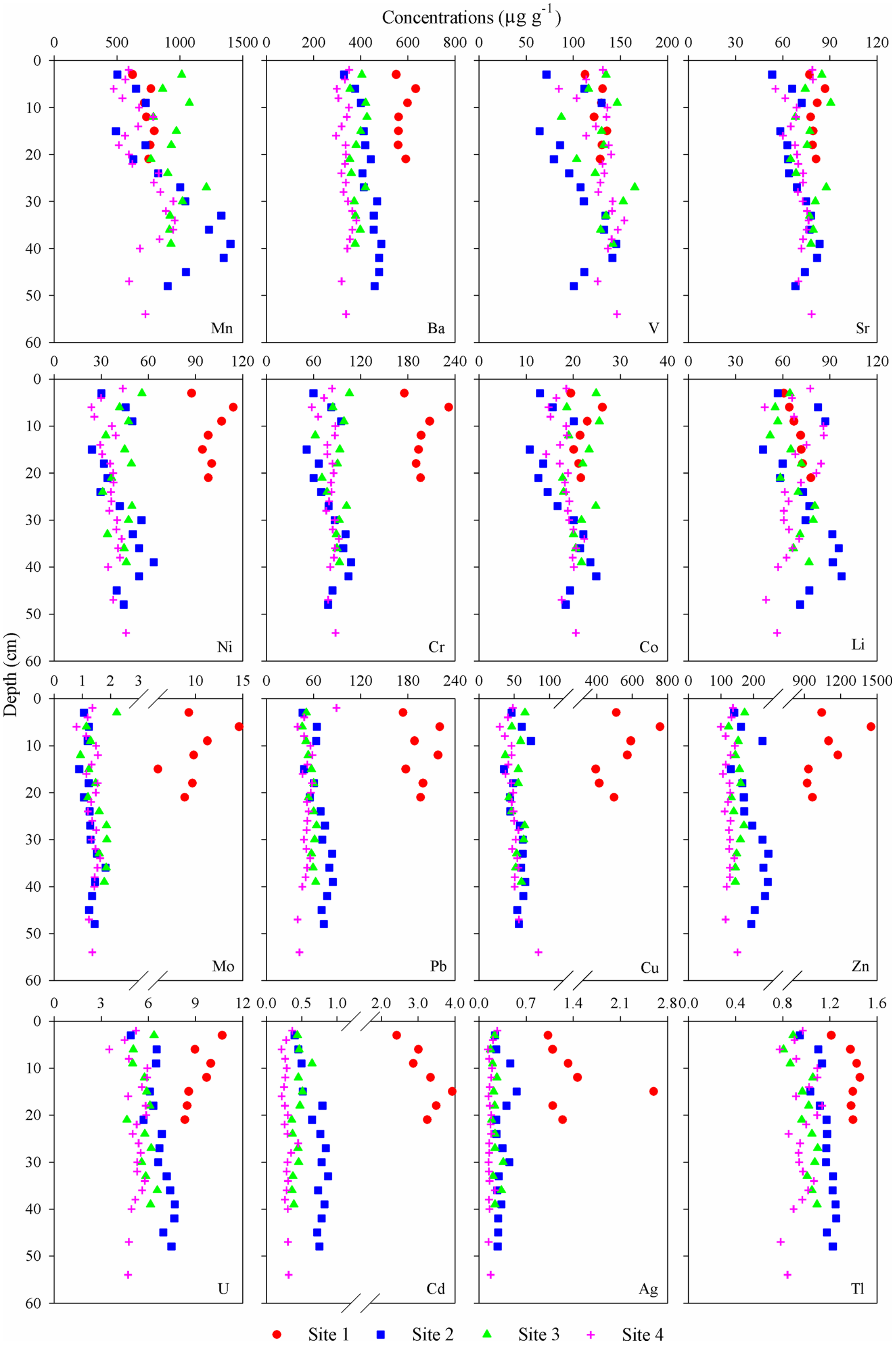

Fig. 4 Vertical profiles of trace elements and Mn in the sediments from the Pearl River and estuary

Table 5 Summary of trace elements and Mn in the four sediment cores from the Pearl River and estuary

Sites		Mn	Ba	V	Sr	Cr	Co	Ni	Cu	Zn	Pb	Li	Mo	U	Cd	Ag	Tl
1	Min.	625	551	113	77.1	176	19.5	87.6	393	924	174	60.8	6.02	8.33	2.42	1.03	1.21
HP	Max.	797	633	136	87.0	232	26.2	114	758	1450	221	78.0	14.6	10.7	3.92	2.59	1.45
	Mean	738	579	127	80.5	199	21.9	99.9	534	1090	197	69.4	9.93	9.25	3.19	1.41	1.38
2	Min.	492	329	64.4	53.3	51.2	10.8	24.1	35.4	130	45.9	47.5	0.89	4.87	0.40	0.24	0.94
NZ	Max.	1400	487	146	83.5	108	24.9	63.4	73.7	245	84.5	97.4	1.82	7.69	0.87	0.56	1.25
	Mean	925	432	108	69.8	81.6	17.8	43.2	55.6	196	68.0	76.1	1.29	6.70	0.69	0.33	1.16
3	Min.	770	353	87.3	65.0	62.2	17.7	30.8	37.4	123	45.6	51.9	0.94	4.64	0.36	0.17	0.81
HM	Max.	1210	427	165	90.6	106	25.5	56.0	65.4	173	63.9	80.3	2.22	6.57	0.65	0.36	1.10
	Mean	948	388	131	77.5	88.4	21.4	43.1	54.1	150	56.6	66.8	1.54	5.76	0.44	0.24	0.99
4	Min.	473	295	84.7	55.3	57.6	14.3	23.8	29.5	99.2	39.6	48.5	0.79	3.51	0.21	0.13	0.77
NLD	Max.	959	381	154	79.2	92.1	22.3	45.8	84.3	151	89.2	86.1	1.63	5.94	0.45	0.27	1.13
	Mean	712	336	131	70.6	81.1	18.4	36.4	48.8	125	52.0	67.5	1.35	5.20	0.29	0.17	0.96
(1)	Mean	474	164	95	NA	71	12	34	41	163	67	51	NA	NA	NA	NA	NA
(2)	Mean	NA	NA	NA	NA	66.8	NA	26.8	20.5	150	41.8	NA	NA	NA	0.45	NA	NA
(3)	Mean	NA	NA	NA	NA	63.7	NA	NA	253.6	370	95.5	NA	NA	NA	1.44	NA	NA
(4)	Mean	1034	502	140	86.3	87.4	19.1	43.4	54.1	206	79.6	36.0	2.42	4.78	NA	NA	NA
(5)	Mean	960	410	103	62.9	65.3	15.0	34.7	62.1	203	118.1	41.9	2.30	6.17	NA	NA	NA
(6)	Mean	646	415	89	51.7	58.1	14.0	34.0	43.3	196	89.4	43.1	2.80	8.81	NA	NA	NA
(7)	Mean	508	168	90.1	29.0	91.0	11.3	30.2	38.0	123	37.6	61.0	1.0	3.15	1.9	1.1	0.61
(8)	Range	362-1070	NA	NA	NA	29.0-104	8.0-35.5	12.0-77.6	9.0-187	45.0-213	10.0-69	37.0-85.2	NA	NA	NA	NA	NA
(9)	ERL	NA	NA	NA	NA	81	NA	20.9	34	150	46.7	NA	NA	NA	1.2	1.0	NA
(10)	ERM	NA	NA	NA	NA	370	NA	51.6	270	410	218	NA	NA	NA	9.6	3.7	NA
(11)	Baseline	600	550	107	350	83	17	44	25	71	17	20	1.5	2.8	0.098	0.05	0.75

All values in micrograms per gram

Medway Estuary (Reid and Spencer 2009) (*1*), Gironde Estuary (Larrose et al. 2010) (*2*), The Pearl River (Wang et al. 2011) (*3*), The West River in the Pearl River system (Zhang and Wang 2001) (*4*), The North River in the Pearl River system (Zhang and Wang 2001) (*5*), The East River in the Pearl River system (Zhang and Wang 2001) (*6*), The Pearl River Estuary (Woods et al. 2012) (*7*) and (Qi et al. 2010) (*8*), NOAA Screening Quick Reference Tables (Buchman 2008) (*9*) and (*10*), and Average upper crust (McLennan 2001) (*11*)

NA not available

the estuarine environment was seawater; the marine source of Na also showed a strong relationship with Mg and K (Spencer 2002). Previous studies in the Pearl River Estuary had also showed that the distribution of Mg and Ca may reflect the combined effects of parent material influences and sedimentation processes in the interaction with marine water (Li et al. 2000; Liu et al. 2003). Na had a strong positive correlation with Mg and a negative correlation with K in this study (Table 6). An examination of the K data revealed an impoverishment of K in estuary sediments and a relative enrichment in river sediments, which was contrary to Na data (Fig. 2), suggesting that there may be an additional anthropogenic source of K in the study area.

Factor 2, which is typically indicative of a marine source, was dominated by Na, Mg, Ti, V, and Ca. Generally, an opposite relationship between the anthropogenic metals (fluvially/terrestrially derived) and Na (marine-derived) would be expected (Spencer 2002). Therefore, K, Cd, Ag, Ba, Tl, Zn, U, and Pb may be derived from anthropogenic sources. It is noteworthy that Ba, Tl, Zn, U, and Pb had strong or moderate loadings both on factor 1 and/or factor 2, indicating that these trace elements were derived both from lithogenic and anthropogenic sources, while K, Cd, and Ag were primarily derived from anthropogenic sources.

Enrichment factor

The first but crucial step for *EF* calculations is to select the reference element and the background values. Typically, Al is considered as an appropriate element to normalize the metal contents because it is a conservative element and one of the most abundant elements

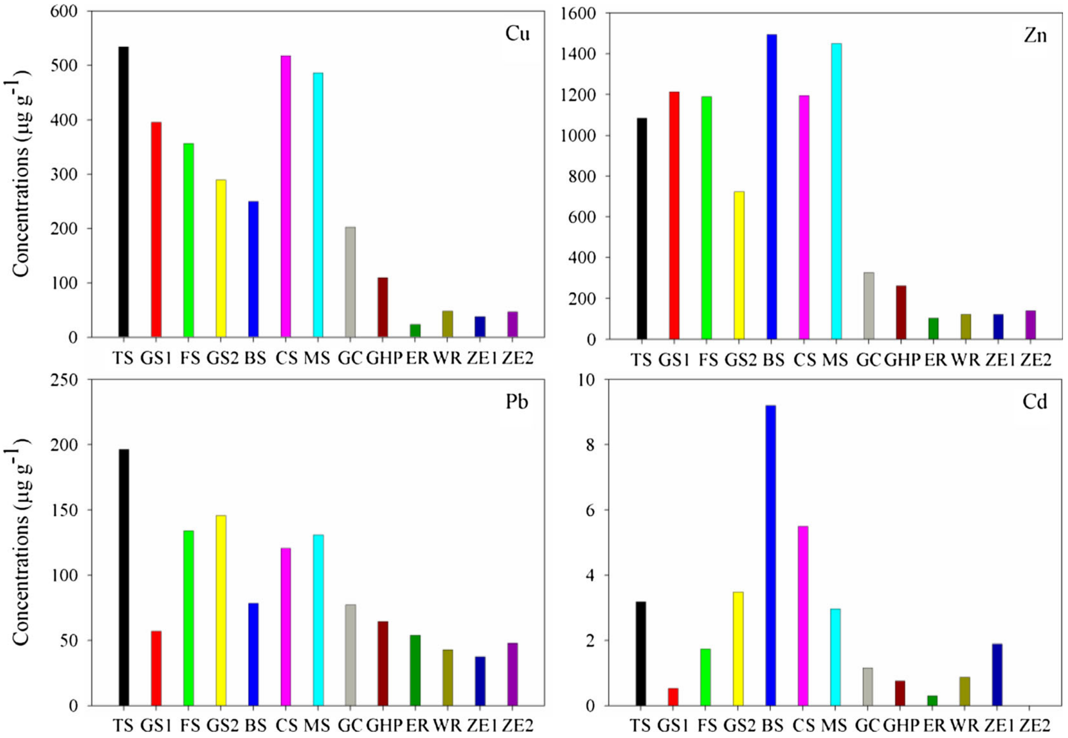

Fig. 5 Comparison of heavy metal concentrations in different samples. *TS* this study (site 1), *GS1* (Cai et al. 2007) and *GS2* (C.S. Zhang et al. 2011) sewage sludge of Guangzhou, *FS* sewage sludge of Foshan (Cai et al. 2007), *BS* sewage sludges of Beijing (Dai et al. 2007), *CS* sewage sludge of Changsha (Yuan et al. 2011), *MS* sewage sludge of China (T. B. Chen et al. 2003), *GC* and *GHP* sediment from the Pearl River (Wang et al. 2011), *ER* and *WR* sediments from East River and West River (G. H. Zhou et al. 2013), *ZE1* (Woods et al. 2012) and *ZE2* (Ip et al. 2007) sediments from Pearl River Estuary. There were no data for Cd in ZE2

on the earth, usually with no contamination. In this study, aluminum was better correlated with trace metals than Fe, suggesting that Al was the main geochemical carrier in the studied sediments. The world average shale and the upper continental crust are often used to provide background metal levels, which allow comparison with the values obtained in the studied areas, as well as with the *EF* reported in other estuarine areas (Celis-Hernandez et al. 2013). However, these metal levels tend to be very general and may be misleading in a specific coastal area (Gibbs 1993). The regional background values would be more appropriate and reliable, but it is difficult to ascertain the regional preindustrial sediment data. Therefore, *EFs* were calculated using Al and three background values (regional background values (Qi et al. 2010), the upper crust for Central East China (UCCEC) (Gao et al. 1998) and the upper crust for the world (UCW) (McLennan 2001)), with the purpose of comparing the effect of different background values. It should be noted that the regional background values used were lacking data for some trace metals (i.e., Mo, U, Cd, Ag, and Tl), which may often occur when using regional background values to calculate the *EFs*.

The *EFs* using regional background values were 0.5–1.3 for EF_{Cr}, 0.3–0.6 for EF_{Co}, 0.4–1.4 for EF_{Ni}, 0.6–9.7 for EF_{Cu}, 0.6–6.1 for EF_{Zn}, 0.7–3.1 for EF_{Pb}, and 0.3–0.5 for EF_{Li}, suggesting that Cr, Co, Ni, and Li may be entirely from crustal materials or natural weathering processes (Table 7). In contrast, the higher average of EF_{Cu} (7.2), EF_{Zn} (4.8), and EF_{Pb} (2.7) at site 1 suggests that these metals were moderately or significantly polluted. Comparing these metal values with effects range low and effects range median (Table 5), it can be concluded that site 1 was severely polluted by Cu, Zn, and Pb. Moreover, moderate pollution was found using the average EF_{Zn} (4.8) and EF_{Pb} (2.7) based on the regional background values. EF_{Co}, EF_{Ni}, EF_{Zn}, EF_{Cd}, and EF_{Li} were comparable between the two crust-referenced *EFs*, whereas EF_{Cu}, EF_{Pb}, EF_{Mo}, EF_{U}, EF_{Ag}, and EF_{Tl} were relatively different. Specifically, EF_{Cu}, EF_{Pb}, and EF_{Ag} were higher based on the UCW than those based on the

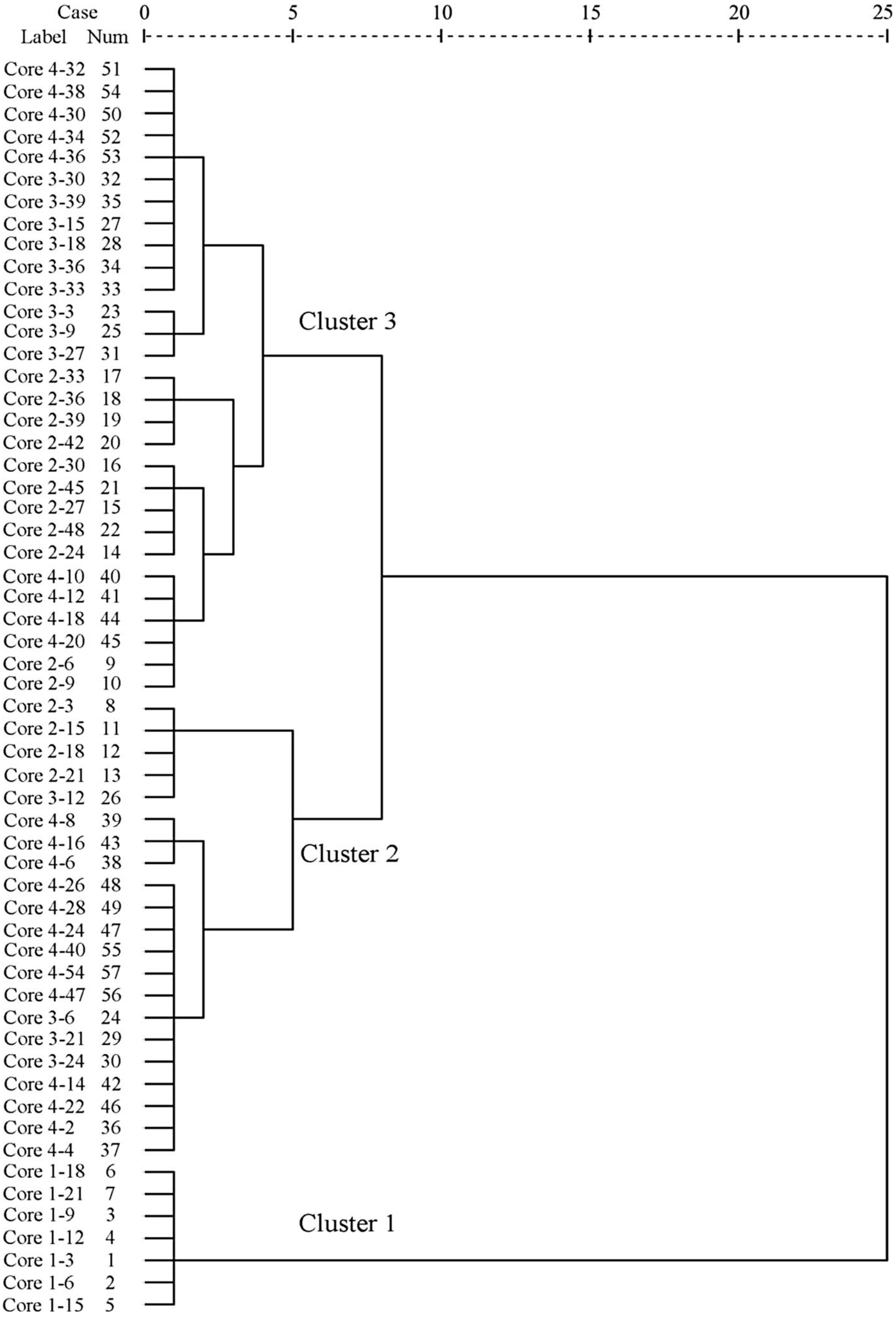

Fig. 6 Dendrogram showing clustering of subsamples in the four cores. Label (Core 4–32): the 4 and 32 represent the sampling sites and the sample depth, respectively

UCCEC. However, EF_{Mo}, EF_U, and EF_{Tl} were reversed. As illustrated by the PCA, Cu mostly originated from a natural source; U and Tl were partially derived from anthropogenic sources. In view of these conflicting features, selecting an appropriate background value is essential for obtaining reliable *EFs*. Other research has also shown that *EF* values will change considerably with different baseline values (Abrahim and Parker 2008; Celis-Hernandez et al. 2013). Consequently, it is more logical and appropriate to use the UCCEC for normalization than to use regional background values or the UCW.

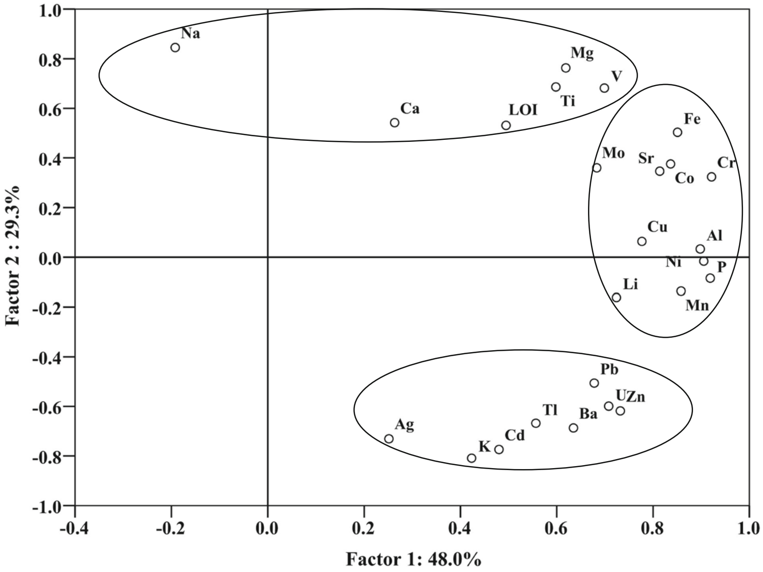

Fig. 7 Principal component score plots of major and trace elements in sediment cores. Data are obtained from the subsamples of cores 2, 3, and 4

The results obtained using the UCCEC demonstrate that high *EF* values (e.g., 25 for Cd and Ag, 14 for Cu, 12 for Zn and Mo, 7.0 for Pb, and 4.7 for U) were found at site 1 (Table 7), while *EF* values for these metals were significantly lower at sites 2, 3, and 4. In contrast, the average *EF* value for Co at site 1 was comparable with its values at other sites, suggesting that sewage discharges or sludge may not be the primary sources for Co compared with Cu, Zn, Pb, Cr, Ni, and Cd. Specifically, the average EF_{Cd} (21) at site 1 was larger than 20, indicating that Cd contamination was very high. The average *EF* values for Ag, Cu, Zn, Mo, and Pb at site 1 and for Cd at site 2 were between 5 and 20, suggesting significant contamination of these metals. The majority of the remaining *EF* values were less than 5, and some were even less than 2, indicating that these metals were at most moderately contaminated.

Comparison of the PCA and *EF*

It is noteworthy that conflicts were observed for some trace elements when comparing the results of PCA, ERL-ERM with *EF*. For example, Li mainly originated from natural sources based on the PCA. However, it was moderately polluted based on the *EF*. On the contrary, Tl primarily originated from anthropogenic sources based on the PCA. However, nearly no pollution was found based on the *EF*. The concentrations of Cd and Ag were lower than the ERM value but exceeded the ERL value at site 1, while it was highly polluted based on the *EF*. These conflicts can be attributed to the background values used in the *EFs*. The average value (18 μg g^{-1}) of Li in the UCCEC was much lower than the minimum value (47.5 μg g^{-1}) in our study. It is also lower than the minimum value (26.8 μg g^{-1}) in surface sediments from the Pearl River Estuary (Woods et al. 2012). However, other trace elements (i.e., Cr, Co, Ni, Cu, Zn, Pb, Cd, and Tl) were higher in the UCCEC compared with the relevant minimum values in the same literature (Woods et al. 2012). In the case of Tl, the minimum value (0.18 μg g^{-1}) in surface sediments from the Pearl River Estuary (Woods et al. 2012) was approximately 43 % of the UCCEC content (0.42 μg g^{-1}) (Gao et al. 1998). Therefore, the low background value of Li and the high background value of Tl may result in the high and the low *EFs* of Li and Tl, respectively. It is important to note that selecting the background values for normalization should consider the existing data in the study area (including the core samples and/or the unpolluted surface sediment samples) and the regional and worldwide average values in shales and/or continental crusts. Furthermore, carefully comparing these data to determine the combined background values, which may be more appropriate and logical than single-source background values, is necessary.

Table 6 Pearson's correlation coefficients (*r*) between major and trace elements in cores 2, 3, and 4 ($n=50$)

	Al	Fe	K	Mg	Na	Ca	Ti	P	LOI[c]	Mn	Ba	V	Sr	Li	Cr	Co	Ni	Cu	Zn	Pb	Cd	Ag	Tl	Mo
Fe	0.799[a]																							
K	0.312[b]	−0.033																						
Mg	0.628[b]	0.919[a]	−0.363[a]																					
Na	−0.041	0.276	−0.711[a]	0.570[a]																				
Ca	−0.022	0.452[a]	−0.272	0.506[a]	0.169																			
Ti	0.439[a]	0.838[a]	−0.240	0.857[a]	0.374[a]	0.725[a]																		
P	0.820[a]	0.733[a]	0.467[a]	0.501[a]	−0.215	0.178	0.469[a]																	
LOI	0.705[a]	0.707[a]	−0.331[b]	0.767[a]	0.531[a]	0.021	0.416[a]	0.430[a]																
Mn	0.696[a]	0.680[a]	0.463[a]	0.397[a]	−0.424[a]	0.269	0.502[a]	0.712[a]	0.214															
Ba	0.469[a]	0.193	0.922[a]	−0.159	−0.748[a]	−0.055	0.007	0.615[a]	−0.213	0.712[a]														
V	0.712[a]	0.944[a]	−0.269	0.972[a]	0.472[a]	0.474[a]	0.869[a]	0.572[a]	0.780[a]	0.496[a]	−0.039													
Sr	0.603[a]	0.853[a]	0.142	0.748[a]	0.076	0.684[a]	0.837[a]	0.696[a]	0.360[b]	0.712[a]	0.396[a]	0.773[a]												
Li	0.869[a]	0.555[a]	0.315[b]	0.403[a]	−0.126	−0.227	0.089	0.690[a]	0.642[a]	0.489[a]	0.392[a]	0.444[a]	0.334[b]											
Cr	0.825[a]	0.943[a]	0.107	0.813[a]	0.076	0.424[a]	0.777[a]	0.844[a]	0.599[a]	0.746[a]	0.356[b]	0.852[a]	0.850[a]	0.625[a]										
Co	0.662[a]	0.919[a]	0.124	0.785[a]	0.085	0.546[a]	0.842[a]	0.703[a]	0.440[a]	0.768[a]	0.365[a]	0.807[a]	0.894[a]	0.385[a]	0.898[a]									
Ni	0.721[a]	0.743[a]	0.419[a]	0.522[a]	−0.205	0.274	0.569[a]	0.871[a]	0.338[b]	0.769[a]	0.601[a]	0.578[a]	0.755[a]	0.551[a]	0.860[a]	0.789[a]								
Cu	0.592[a]	0.655[a]	0.263	0.477[a]	−0.165	0.335[b]	0.573[a]	0.786[a]	0.328[b]	0.596[a]	0.428[a]	0.567[a]	0.658[a]	0.394[a]	0.735[a]	0.658[a]	0.809[a]							
Zn	0.605[a]	0.310[b]	0.781[a]	−0.030	−0.688[a]	−0.142	−0.007	0.754[a]	0.034	0.710[a]	0.875[a]	0.073	0.382[a]	0.629[a]	0.493[a]	0.393[a]	0.710[a]	0.609[a]						
Pb	0.664[a]	0.326[b]	0.612[a]	0.088	−0.460[a]	−0.225	−0.045	0.626[a]	0.233	0.597[a]	0.694[a]	0.147	0.340[b]	0.761[a]	0.438[a]	0.302[b]	0.577[a]	0.362[a]	0.781[a]					
Cd	0.302[b]	−0.002	0.791[a]	−0.328[b]	−0.834[a]	−0.114	−0.174	0.480[a]	−0.278	0.611[a]	0.879[a]	−0.208	0.206	0.348[b]	0.203	0.156	0.466[a]	0.369[a]	0.857[a]	0.703[a]				
Ag	0.143	−0.171	0.715[a]	−0.387[a]	−0.652[a]	−0.169	−0.298[b]	0.321[b]	−0.348[b]	0.226	0.649[a]	−0.318[b]	0.031	0.218	−0.014	−0.084	0.265	0.251	0.615[a]	0.492[a]	0.633[a]			
Tl	0.659[a]	0.159	0.770[a]	−0.121	−0.543[a]	−0.453[a]	−0.237	0.541[a]	0.164	0.484[a]	0.745[a]	−0.002	0.091	0.738[a]	0.255	0.114	0.393[a]	0.256	0.757[a]	0.795[a]	0.676[a]	0.562[a]		
Mo	0.657[a]	0.745[a]	−0.009	0.673[a]	0.163	0.381[a]	0.645[a]	0.515[a]	0.553[a]	0.512[a]	0.165	0.695[a]	0.630[a]	0.456[a]	0.708[a]	0.641[a]	0.552[a]	0.505[a]	0.211	0.283[b]	−0.011	−0.050	0.231	
U	0.678[a]	0.299[b]	0.772[a]	−0.010	−0.587[a]	−0.241	0.005	0.682[a]	0.084	0.657[a]	0.829[a]	0.098	0.298[b]	0.686[a]	0.460[a]	0.321[b]	0.593[a]	0.455[a]	0.831[a]	0.794[a]	0.756[a]	0.580[a]	0.881[a]	0.375[a]

[a] Correlation is significant at the 0.01 level (two-tailed)

[b] Correlation is significant at the 0.05 level (two-tailed)

[c] Loss on ignition

Table 7 Mean metal enrichment factor values in the four sediment cores from the Pearl River and estuary normalized with respect to the aluminum content in regional background, upper crust for Central East China, and upper continental crust, respectively

	Sampling site		Cr	Co	Ni	Cu	Zn	Pb	Li	Mo	U	Cd	Ag	Tl	Al
Based on regional background	1 *HP*	Range	1.1–1.3	0.4–0.5	1.2–1.4	5.2–9.7	4.0–6.1	2.4–3.1	0.3–0.4						
		Mean	1.2	0.4	1.3	7.2	4.8	2.7	0.4						
	2 *NZ*	Range	0.5–0.6	0.3–0.4	0.5–0.8	0.7–1.0	0.8–1.1	0.9–1.2	0.4–0.5						
		Mean	0.6	0.4	0.6	0.9	1.0	1.1	0.5						
	3 *HM*	Range	0.5–0.8	0.4–0.6	0.5–0.8	0.7–1.1	0.7–1.0	0.8–1.2	0.4–0.5						
		Mean	0.6	0.5	0.6	0.9	0.8	1.0	0.4						
	4 *NLD*	Range	0.5–0.7	0.3–0.5	0.4–0.7	0.6–1.4	0.6–0.8	0.7–1.5	0.4–0.5						
		Mean	0.6	0.4	0.6	0.8	0.7	0.9	0.5						
	Background values[a]		58	18	28	26	79	25	62	NA	NA	NA	NA	NA	4.14
Based on upper crust for Central East China	1	Range	1.4–1.7	0.7–0.8	1.4–1.7	7.2–14	7.9–12	5.5–7.0	1.8–2.4	5.0–12	3.3–4.7	18–25	10–25	1.7–1.9	
	HP	Mean	1.5	0.7	1.5	10	9.3	6.3	2.1	8.4	3.6	21	14	1.8	
	2	Range	0.6–0.8	0.6–0.8	0.6–0.9	1.0–1.4	1.6–2.1	2.1–2.8	2.4–2.8	1.0–1.5	2.6–4.0	3.3–7.1	2.5–9.2	1.4–2.2	
	NZ	Mean	0.7	0.7	0.7	1.2	1.9	2.5	2.6	1.3	3.0	5.2	3.9	1.7	
	3	Range	0.7–1.0	0.7–1.1	0.6–1.0	1.0–1.5	1.3–1.9	1.9–2.7	2.1–2.5	1.2–2.3	2.2–3.5	2.6–5.3	2.2–4.1	1.3–2.1	
	HM	Mean	0.8	0.9	0.8	1.2	1.5	2.2	2.4	1.5	2.7	3.5	2.9	1.5	
	4	Range	0.7–0.9	0.6–0.9	0.5–0.9	0.9–2.0	1.1–1.6	1.7–3.4	2.1–2.9	1.2–1.6	2.3–2.7	1.7–3.6	1.6–3.2	1.4–1.8	
	NLD	Mean	0.8	0.8	0.7	1.1	1.3	2.0	2.5	1.4	2.5	2.3	2.0	1.5	
	Background values[b]		71	16	35	29	63	17	18	0.64	1.39	0.083	0.055	0.42	6.41
Based on upper crust	1	Range	1.5–1.8	0.8–1.0	1.4–1.7	10–20	8.7–13	6.9–8.8	2.1–2.7	2.7–6.3	2.0–2.9	19–27	14–34	1.2–1.3	
	HP	Mean	1.6	0.9	1.5	15	10	7.8	2.4	4.5	2.3	22	19	1.2	
	2	Range	0.7–0.8	0.7–0.9	0.6–0.9	1.5–2.1	1.8–2.4	2.6–3.5	2.7–3.2	0.5–0.8	1.6–2.5	3.5–7.6	3.4–13	1.0–1.6	
	NZ	Mean	0.8	0.8	0.7	1.7	2.1	3.1	2.9	0.7	1.9	5.5	5.4	1.2	
	3	Range	0.7–1.0	0.8–1.3	0.6–1.0	1.5–2.1	1.4–2.2	2.4–3.3	2.4–2.9	0.7–1.2	1.4–2.2	2.8–5.6	3.0–5.7	0.9–1.5	
	HM	Mean	0.9	1.0	0.8	1.7	1.7	2.7	2.7	0.8	1.7	3.7	3.9	1.1	
	4	Range	0.7–0.9	0.7–1.0	0.5–0.9	1.3–2.9	1.2–1.8	2.1–4.2	2.4–3.3	0.6–0.8	1.4–1.7	1.8–3.9	2.2–4.4	1.0–1.2	
	NLD	Mean	0.8	0.9	0.7	1.6	1.5	2.5	2.8	0.7	1.5	2.5	2.8	1.1	
	Background values[c]		83	17	44	25	71	17	20	1.5	2.8	0.098	0.050	0.75	8.04

Background values in percent for Al and in micrograms per gram for other trace metals

NA not available

[a] From Qi et al. (2010)

[b] From Gao et al. (1998)

[c] From McLennan (2001)

Conclusions

The present study showed preliminary but still relevant information regarding the mineralogical and geochemical compositions among sediments in four cores from the Pearl River and estuary. One core (Huangpu) with very high contents of trace elements was identified as heavily polluted based both on sediment quality guidelines (ERL-ERM) and *EFs*. Sewage disposal and/or the surreptitious dumping of sludge was likely the source for the trace elements in this site. Moreover, significant metal pollutions in sediment from the other three sites were not found. Very high pollution for Cd and significant contaminations for Ag, Cu, Zn, Mo, and Pb were identified based on *EFs*. Comparing the *EF* results with the PCA and ERL-ERM results, conflicts are observed for some trace metals, which were attributed to the background values used to compute the *EFs*. Therefore, combined background values may be more appropriate and logical than single-source background values. The multivariate analysis procedures were useful tools for the classification of the pollution levels. Subsamples (Huangpu) were excluded prior to performing the PCA based on cluster analysis, which separated the subsamples (Huangpu) with a distinct single source from others. Continuous monitoring and further studies of the area adjacent to the outlet of the wastewater treatment plant are needed to identify the pollution sources and assess the toxicity of the very high levels of trace metals to the benthic organisms. The authorities should also take forceful measures to prevent the dumping of sludge into the rivers.

Acknowledgments This study was supported by the National Natural Science Foundation of China (No. 40903047) and Chinese Academy of Sciences (No. KZZD-EW-09-2). The authors thank Derong Zhang for the sample collection and Ying Liu, Xueping Liu, and Jingming Wei for the major and trace elements and XRD analyses. The authors are also grateful to the anonymous reviewers for the upgradation of the manuscript. This is contribution No. IS-1936 from GIGCAS.

References

Abrahim, G. M. S., & Parker, R. J. (2008). Assessment of heavy metal enrichment factors and the degree of contamination in marine sediments from Tamaki Estuary, Auckland, New Zealand. *Environmental Monitoring and Assessment, 136*(1–3), 227–238.

Attia, O. E. A., & Ghrefat, H. (2013). Assessing heavy metal pollution in the recent bottom sediments of Mabahiss Bay, North Hurghada, Red Sea, Egypt. *Environmental Monitoring and Assessment, 185*(12), 9925–9934.

Badr, N. B. E., El-Fiky, A. A., Mostafa, A. R., & Al-Mur, B. A. (2009). Metal pollution records in core sediments of some Red Sea coastal areas, Kingdom of Saudi Arabia. *Environmental Monitoring and Assessment, 155*(1–4), 509–526.

Birch, G., Siaka, M., & Owens, C. (2001). The source of anthropogenic heavy metals in fluvial sediments of a rural catchment: Coxs River, Australia. *Water, Air, and Soil Pollution, 126*(1–2), 13–35.

Buchman, M. F. (2008). NOAA Screening Quick Reference Tables. NOAA OR&R Report 08–1, Seattle, Washington. Office of Response and Restoration Division, National Oceanic and Atmospheric Administration. 34 pp.

Cai, Q. Y., Mo, C. H., Wu, Q. T., Zeng, Q. Y., & Katsoyiannis, A. (2007). Concentration and speciation of heavy metals in six different sewage sludge-composts. *Journal of Hazardous Materials, 147*(3), 1063–1072.

Celis-Hernandez, O., Rosales-Hoz, L., & Carranza-Edwards, A. (2013). Heavy metal enrichment in surface sediments from the SW Gulf of Mexico. *Environmental Monitoring and Assessment, 185*(11), 8891–8907.

Chatterjee, M., Silva, E. V., Sarkar, S. K., Sella, S. M., Bhattacharya, A., Satpathy, K. K., et al. (2007). Distribution and possible source of trace elements in the sediment cores of a tropical macrotidal estuary and their ecotoxicological significance. *Environment International, 33*(3), 346–356.

Chen, T. B., Huang, Q. F., Gao, D., Zheng, Y. Q., & Wu, J. F. (2003). Heavy metal concentrations and their decreasing trends in sewage sludges of China. *Acta Scientiae Circumstantiae, 23*(5), 561–569.

Chen, K. P., Jiao, J. J., Huang, J. M., & Huang, R. Q. (2007). Multivariate statistical evaluation of trace elements in groundwater in a coastal area in Shenzhen, China. *Environmental Pollution, 147*(3), 771–780.

Chen, B. W., Liang, X. M., Xu, W. H., Huang, X. P., & Li, X. D. (2012). The changes in trace metal contamination over the last decade in surface sediments of the Pearl River Estuary, South China. *Science of the Total Environment, 439*, 141–149.

Dai, M. H., Guo, X. H., Zhai, W. D., Yuan, L. Y., Wang, B. W., Wang, L. F., Cai, P. H., Tang, T. T., & Cai, W. J. (2006). Oxygen depletion in the upper reach of the Pearl River estuary during a winter drought. *Marine Chemistry, 102*, 159–169.

Dai, J. Y., Xu, M. Q., Chen, J. P., Yang, X. P., & Ke, Z. S. (2007). PCDD/F, PAH and heavy metals in the sewage sludge from six wastewater treatment plants in Beijing, China. *Chemosphere, 66*(2), 353–361.

Du Laing, G., Rinklebe, J., Vandecasteele, B., Meers, E., & Tack, F. M. G. (2009). Trace metal behaviour in estuarine and riverine floodplain soils and sediments: a review. *Science of the Total Environment, 407*(13), 3972–3985.

Filipovic, J., Grcic, I., Bermanec, V., & Kniewald, G. (2013). Monitoring of total metal concentration in sludge samples: case study for the mechanical-biological wastewater treatment plant in Velika Gorica, Croatia. *Science of the Total Environment, 447*, 17–24.

Gao, S., Luo, T. C., Zhang, B. R., Zhang, H. F., Han, Y. W., Zhao, Z. D., et al. (1998). Chemical composition of the continental crust as revealed by studies in East China. *Geochimica Et Cosmochimica Acta, 62*(11), 1959–1975.

Gibbs, R. J. (1993). Metals of the Bottom Muds in Townsville Harbor, Australia. *Environmental Pollution, 81*(3), 297–300.

Gong, W. P., Shen, J., & Jia, L. W. (2013). Salt intrusion during the dry season in the Huangmaohai Estuary, Pearl River Delta, China. *Journal of Marine Systems, 111–112*, 235–252.

Gonzalez-Garcia, S., & Sanchez-Camazano, M. (1968). Differentiation of kaolinite from chlorite by treatment with dimethyl-sulphoxide. *Clay Minerals, 7*, 447–450.

Greger, M., Kautsky, L., & Sandberg, T. (1995). A tentative model of Cd uptake in *Potamogeton pectinatus* in relation to salinity. *Environmental and Experimental Botany, 35*(2), 215–225.

Harikumar, P. S., & Nasir, U. P. (2010). Ecotoxicological impact assessment of heavy metals in core sediments of a tropical estuary. *Ecotoxicology and Environmental Safety, 73*(7), 1742–1747.

He, B. Y., Dai, M. H., Zhai, W. D., Wang, L. F., Wang, K. J., Chen, J. H., et al. (2010). Distribution, degradation and dynamics of dissolved organic carbon and its major compound classes in the Pearl River estuary, China. *Marine Chemistry, 119*, 52–64.

Heise, B., Bobertz, B., & Harff, J. (2010). Classification of the Pearl River Estuary via principal component analysis and regionalisation. *Journal of Coastal Research, 26*(4), 769–779.

Ho, H. H., Swennen, R., Cappuyns, V., Vassilieva, E., Neyens, G., Rajabali, M., et al. (2013). Geogene versus anthropogene origin of trace metals in sediments in Cua Luc Estuary and Ha Long Bay, Vietnam. *Estuaries and Coasts, 36*(1), 203–219.

Ip, C. C. M., Li, X. D., Zhang, G., Wai, O. W. H., & Li, Y. S. (2007). Trace metal distribution in sediments of the Pearl River Estuary and the surrounding coastal area, South China. *Environmental Pollution, 147*(2), 311–323.

Jonathan, M. P., Ram-Mohan, V., & Srinivasalu, S. (2004). Geochemical variations of major and trace elements in recent sediments, off the Gulf of Mannar, the southeast coast of India. *Environmental Geology, 45*(4), 466–480.

Kalnejais, L. H., Martin, W. R., & Bothner, M. H. (2010). The release of dissolved nutrients and metals from coastal sediments due to resuspension. *Marine Chemistry, 121*(1–4), 224–235.

Larrose, A., Coynel, A., Schafer, J., Blanc, G., Masse, L., & Maneux, E. (2010). Assessing the current state of the Gironde Estuary by mapping priority contaminant distribution and risk potential in surface sediment. *Applied Geochemistry, 25*(12), 1912–1923.

Lavilla, I., Filgueiras, A. V., Valverde, F., Millos, J., Palanca, A., & Bendicho, C. (2006). Depth profile of trace elements in a sediment core of a high-altitude lake deposit at the Pyrenees, Spain. *Water, Air, and Soil Pollution, 172*(1–4), 273–293.

Li, X. D., Wai, O. W. H., Li, Y. S., Coles, B. J., Ramsey, M. H., & Thornton, I. (2000). Heavy metal distribution in sediment profiles of the Pearl River estuary, South China. *Applied Geochemistry, 15*(5), 567–581.

Liu, W. X., Li, X. D., Shen, Z. G., Wang, D. C., Wai, O. W. H., & Li, Y. S. (2003). Multivariate statistical study of heavy metal enrichment in sediments of the Pearl River Estuary. *Environmental Pollution, 121*(3), 377–388.

Loizeau, J.-L., Pardos, M., Monna, F., Peytremann, C., Haller, L., & Dominik, J. (2004). The impact of a sewage treatment plant's effluent on sediment quality in a small bay in Lake Geneva (Switzerland–France). Part 2: temporal evolution of heavy metals. *Lakes & Reservoirs: Research & Management, 9*(1), 53–63.

Luo, J. H. (2002). The analysis of the primary cause of the low dissolved oxygen of the partial water body in the Guangzhou reach of the Pearl River. *Research of Environmental Sciences, 15*, 8–11 (in chinese).

Mai, B. X., Fu, J. M., Zhang, G., Lin, Z., Min, Y. S., Sheng, G. Y., et al. (2001). Polycyclic aromatic hydrocarbons in sediments from the Pearl river and estuary, China: spatial and temporal distribution and sources. *Applied Geochemistry, 16*, 1429–1445.

Matthai, C., Birch, G. F., & Bickford, G. P. (2002). Anthropogenic trace metals in sediment and settling particulate matter on a high-energy continental shelf (Sydney, Australia). *Marine Environmental Research, 54*(2), 99–127.

McLennan, S. M. (2001). Relationships between the trace element composition of sedimentary rocks and upper continental crust. *Geochemistry Geophysics Geosystems, 2*, art. no.-2000GC000109.

NFDaily (2012). Nanfang Daily. Available at: http://epaper.nfdaily.cn/html/2012-07/31/content_7109145.htm (in chinese).

Pan, K., & Wang, W. X. (2012). Trace metal contamination in estuarine and coastal environments in China. *Science of the Total Environment, 421*, 3–16.

Qi, S., Leipe, T., Rueckert, P., Di, Z., & Harff, J. (2010). Geochemical sources, deposition and enrichment of heavy metals in short sediment cores from the Pearl River Estuary, Southern China. *Journal of Marine Systems, 82*, S28–S42.

Reid, M. K., & Spencer, K. L. (2009). Use of principal components analysis (PCA) on estuarine sediment datasets: the effect of data pre-treatment. *Environmental Pollution, 157*(8–9), 2275–2281.

Seddique, A. A., Masuda, H., Mitamura, M., Shinoda, K., Yamanaka, T., Nakaya, S., & Ahmed, K. M. (2011). Mineralogy and geochemistry of shallow sediments of Sonargaon, Bangladesh and implications for arsenic dynamics: focusing on the role of organic matter. *Applied Geochemistry, 26*, 587–599.

Simeonov, V., Massart, D. L., Andreev, G., & Tsakovski, S. (2000). Assessment of metal pollution based on multivariate statistical modeling of 'hot spot' sediments from the Black Sea. *Chemosphere, 41*(9), 1411–1417.

Spencer, K. L. (2002). Spatial variability of metals in the inter-tidal sediments of the Medway Estuary, Kent, UK. *Marine Pollution Bulletin, 44*(9), 933–944.

Sutherland, R. A. (2000). Bed sediment-associated trace metals in an urban stream, Oahu, Hawaii. *Environmental Geology, 39*(6), 611–627.

Tue, N. T., Quy, T. D., Amano, A., Hamaoka, H., Tanabe, S., Nhuan, M. T., et al. (2012). Historical profiles of trace element concentrations in mangrove sediments from the Ba Lat Estuary, Red River, Vietnam. *Water, Air, and Soil Pollution, 223*(3), 1315–1330.

Varol, M. (2011). Assessment of heavy metal contamination in sediments of the Tigris River (Turkey) using pollution indices and multivariate statistical techniques. *Journal of Hazardous Materials, 195*, 355–364.

Wand, X. L., & Li, Y. (2011). Measurement of Cu and Zn adsorption onto surficial sediment components: new evidence for less importance of caly minerals. *Journal of Hazardous Materials, 189*, 719–723.

Wang, S. L., Lin, C. Y., & Cao, X. Z. (2011). Heavy metals content and distribution in the surface sediments of the Guangzhou section of the Pearl River, Southern China. *Environmental Earth Sciences, 64*(6), 1593–1605.

Woods, A. M., Lloyd, J. M., Zong, Y. Q., & Brodie, C. R. (2012). Spatial mapping of Pearl River Estuary surface sediment geochemistry: influence of data analysis on environmental interpretation. *Estuarine, Coastal and Shelf Science, 115*, 218–233.

Yin, K. D., Lin, Z. F., & Ke, Z. Y. (2004). Temporal and spatial distribution of dissolved oxygen in the Pearl River Estuary and adjacent coastal waters. *Continetal Shelf Research, 24*(16), 1935–1948.

Yu, X. J., Yan, Y., & Wang, W. X. (2010). The distribution and speciation of trace metals in surface sediments from the Pearl River Estuary and the Daya Bay, Southern China. *Marine Pollution Bulletin, 60*(8), 1364–1371.

Yu, X. J., Li, H. X., Pan, K., Yan, Y., & Wang, W. X. (2012). Mercury distribution, speciation and bioavailability in sediments from the Pearl River Estuary, Southern China. *Marine Pollution Bulletin, 64*(8), 1699–1704.

Yuan, X. Z., Huang, H. J., Zeng, G. M., Li, H., Wang, J. Y., Zhou, C. F., et al. (2011). Total concentrations and chemical speciation of heavy metals in liquefaction residues of sewage sludge. *Bioresource Technology, 102*(5), 4104–4110.

Zhang, C. S., & Wang, L. J. (2001). Multi-element geochemistry of sediments from the Pearl River system, China. *Applied Geochemistry, 16*(9–10), 1251–1259.

Zhang, C. S., Chen, Q. L., Zhang, K. F., & Li, S. G. (2011). Chemical forms and bioavailability of heavy metals in the sludge of Datansha Wastewater Treatment Plant. *Journal of Agro-Environment Science, 27*(3), 1259–1264.

Zhou, H. Y., Yin, X. J., Yang, Q. H., Wang, H., Wu, Z. J., & Bao, S. X. (2009). Distribution, source and flux of methane in the western Pearl River Estuary and northern South China Sea. *Marine Chemistry, 117*(1–4), 21–31.

Zhou, G. H., Sun, B. B., Zeng, D. M., Wei, H. L., Liu, Z. Y., & Zhang, B. M. (2013). Vertical distribution of trace elements in the sediment cores from major rivers in east China and its implication on geochemical background and anthropogenic effects. *Journal of Geochemical Exploration*. doi:10.1016/j.gexplo.2013.1003.1007.